ISSN 1674-1056
http://cpb.iphy.ac.cn
http://iopscience.iop.org/cpb
中国物理 B
Chinese Physics
中国物理 Chinese Physics B

Multinary diamond-like chalcogenides for promising thermoelectric application

Dan Zhang(张旦), Hong-Chang Bai(白洪昌), Zhi-Liang Li(李志亮), Jiang-Long Wang(王江龙), Guang-Sheng Fu(傅广生), Shu-Fang Wang(王淑芳)
Citation: Chin. Phys. B . 2018, 27(4): 047206. **doi:** 10.1088/1674-1056/27/4/047206

Journal homepage: http://cpb.iphy.ac.cn; http://iopscience.iop.org/cpb

What follows is a list of articles you may be interested in

Band engineering and precipitation enhance thermoelectric performance of SnTe with Zn-doping

Zhiyu Chen(陈志禹), Ruifeng Wang(王瑞峰), Guoyu Wang(王国玉), Xiaoyuan Zhou(周小元), Zhengshang Wang(王正上), Cong Yin(尹聪), Qing Hu(胡庆), Binqiang Zhou(周斌强), Jun Tang(唐军), Ran Ang(昂然)
Chin. Phys. B . 2018, 27(4): 047202. **doi:** 10.1088/1674-1056/27/4/047202

Synthesis and thermoelectric properties of Nd-single filled p-type skutterudites

Hong Wu(吴宏), Nusrat Shaheen, Heng-Quan Yan(杨恒全), Kun-Ling Peng(彭坤岭), Xing-Chen Shen(沈星辰), Guo-Yu Wang(王国玉), Xu Lu(卢旭), Xiao-Yuan Zhou(周小元)
Chin. Phys. B . 2018, 27(4): 047203. **doi:** 10.1088/1674-1056/27/4/047203

Biaxial strain-induced enhancement in the thermoelectric performance of monolayer WSe_2

Wanhuizi Shen(沈婉慧子), Daifeng Zou(邹代峰), Guozheng Nie(聂国政), Ying Xu(许英)
Chin. Phys. B . 2017, 26(11): 117202. **doi:** 10.1088/1674-1056/26/11/117202

Optimize the thermoelectric performance of CdO ceramics by doping Zn

Xin-Yu Zha(查欣雨), Lin-Jie Gao(高琳洁), Hong-Chang Bai(白洪昌), Jiang-Long Wang(王江龙), Shu-Fang Wang(王淑芳)
Chin. Phys. B . 2017, 26(10): 107202. **doi:** 10.1088/1674-1056/26/10/107202

Thermoelectric properties of Li-doped $Sr_{0.7}Ba_{0.3}Nb_2O_{6-\delta}$ ceramics

Ya-Cui Zhang(张亚翠), Jian Liu(刘剑), Yi Li(李宜), Yu-Fei Chen(陈宇飞), Ji-Chao Li(李吉超), Wen-Bin Su(苏文斌), Yu-Cheng Zhou(周昱成), Jin-Ze Zhai(翟近泽), Teng Wang(王腾), Chun-Lei Wang(王春雷)
Chin. Phys. B . 2017, 26(10): 107201. **doi:** 10.1088/1674-1056/26/10/107201

TOPICAL REVIEW — Recent advances in thermoelectric materials and devices

Multinary diamond-like chalcogenides for promising thermoelectric application*

Dan Zhang(张旦), Hong-Chang Bai(白洪昌), Zhi-Liang Li(李志亮),
Jiang-Long Wang(王江龙), Guang-Sheng Fu(傅广生), and Shu-Fang Wang(王淑芳)†

Hebei Key Laboratory of Optic-Electronic Information and Materials, College of Physics Science and Technology, Hebei University, Baoding 071002, *China*

(Received 30 November 2017; revised manuscript received 3 January 2018; published online 10 March 2018)

Thermoelectric (TE) materials have been considered as a strong candidate for recovering the waste heat from industry and vehicles due to the ability to convert heat directly into electricity. Recently, multinary diamond-like chalcogenides (MDLCs), such as $CuInTe_2$, Cu_2SnSe_3, Cu_3SbSe_4, $Cu_2ZnSnSe_4$, etc., are eco-friendly Pb-free TE materials with relatively large Seebeck coefficient and low thermal conductivity and have aroused intensive research as a popular theme in the TE field. In this review, we summarize the TE performance and device development of MDLCs. The features of crystalline and electronic structure are first analyzed, and then the strategies that have emerged to enhance the TE figure of merits of these materials are illustrated in detail. The final part of this review describes the advance in TE device research for MDLCs. In the outlook, the challenges and future directions are also discussed to promote the further development of MDLCs TE materials.

Keywords: thermoelectric, multinary diamond-like chancogenides, decoupling, electrical and thermal transport properties

PACS: 72.20.Pa, 73.50.Lw **DOI:** 10.1088/1674-1056/27/4/047206

1. Introduction

The ever-growing concern around the energy crisis and environmental pollution have motivated scientists to study and design alternative energy technologies.[1,2] Thermoelectric (TE) materials, which can directly convert heat into electricity or *vice versa*, have received a great deal of attention as a robust candidate for the waste heat recovery and solid state refrigeration. Its efficiency depends on the figure of merit, $zT = S^2\sigma T/\kappa$, where S is the Seebeck coefficient, σ is the electrical conductivity, T is the absolute temperature, and $\kappa(=\kappa_e+\kappa_L)$ is the thermal conductivity. Large S, high σ, and low κ are desired for getting high performance TE material with a high zT value. However, the inherent coupling effects among the S, σ, and κ_e by the carrier concentration make the improvement of zT value extremely difficult.[3–5] Recently, new concepts (e.g., resonant levels,[6] band convergence,[7] multiple filling,[8] hierarchical architecture scattering,[9] and nanomagnets-embedding[10]) are continually put forward to decouple these interrelated parameters, and extremely high zT values are realized in leading materials of PbTe (≥ 2.2) and $CoSb_3$ (≥ 1.8). However, hazardous elements or rare earth elements in these high efficiency TE materials will hamper their wide-scale commercial application. Hence, exploring alternative materials with eco-friendly and earth-abundant elements is one of the hottest areas for researchers in the TE field.[11–13]

Multinary diamond-like chalcogenide (MDLC), such as ternary I–III–VI_2, I_2–IV–VI_3, I_3–V–VI_4 compounds, and quaternary I_2–II–IV–VI_4 compounds (Fig. 1(a)), features the diamond-like structure with deformed tetrahedron building blocks.[14] Most of diamond-like chalcogenides, for example, $Cu(In,Ga)(S,Se)_2$,[15] are well recognized as promising candidates for thin film solar cells, photovoltaic devices, etc., while little attention has been paid to its TE performance. Although the possibilities of MDLCs to be thermoelectric materials have been considered historically,[16–18] their good TE properties at high temperature are not demonstrated due to the difficulties in measuring or synthesizing them. Up to 2009, Pb-free earth-abundant $Cu_2ZnSnSe_4$ compound with diamond-like structure has been discovered to possess relatively high zT value (~ 0.9 at 850 K) after being substituted by Cu or In.[19,20] After that, many diamond-like chalcogenides have been investigated with great interest as promising TE materials and the development of MDLCs can be reflected from the time dependent zT value in Fig. 1(b).[19–67] The zT value up to 1.26 (at 673 K) could be obtained for Bi–Sn codoped Cu_3SbSe_4,[59] the zT value in the (Ag, In)-dual-doped Cu_2SnSe_3 sample approached 1.42 at 823 K,[48] and that of $CuInTe_2$ could increase up to a value as high as 1.61 through integrating the anion substitution and nanoinclusions,[26] moreover, an output power of 0.06 W under a temperature difference of 520 K was obtained for MDLCs thermoelectric module,[35] which reveals that MDLCs with nontoxic components are very promising and even comparable to other state-of-the-art TE materials.

*Project supported by the National Natural Science Foundation of China (Grant Nos. 51372064 and 61704044) and the Key Project of the Natural Science Foundation of Hebei Province, China (Grant No. E2017201227).

†Corresponding author. E-mail: sfwang@hbu.edu.cn

© 2018 Chinese Physical Society and IOP Publishing Ltd

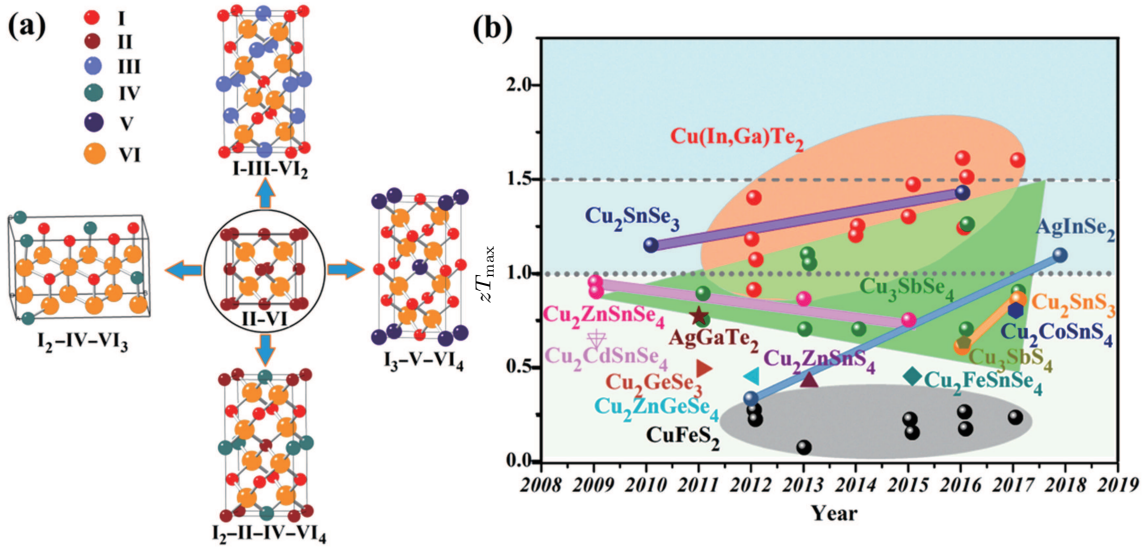


Fig. 1. (color online) (a) Different crystal structures of multinary diamond-like chalcogenides (MDLCs) derived from cubic zincblende structure; (b) timeline for thermoelectric bulk materials with diamond-like structures, showing data from Cu(In, Ga)Te_2,[21–32] $AgGaTe_2$,[33] $AgInSe_2$,[34,35] $CuFeS_2$,[36–44] Cu_2SnS_3,[45,46] Cu_2GeSe_3,[47] Cu_2SnSe_3,[48,49] Cu_3SbS_4,[50] Cu_3SbSe_4,[51–60] Cu_2ZnSnS_4,[61] $Cu_2ZnSnSe_4$,[19,20,62,63] $Cu_2ZnGeSe_4$,[64] $Cu_2CdSnSe_4$,[65] $Cu_2FeSnSe_4$,[66] and Cu_2CoSnS_4.[67]

In this review, we first analyze the crystalline and electronic structure properties of MDLCs briefly, and then the strategies for improving the TE properties of MDLCs are described in detail, including carrier concentration regulation, band structure engineering, the decrease of κ_L and synergistic regulation. Finally, challenges and directions for this type of semiconductor in future commercial applications are also discussed.

2. Crystalline and electronic band structure

MDLCs and their analogies can be taken as derivatives from cubic zincblende binary II–VI compounds (like ZnSe) through orderly substitution of II atoms with the same number of I + III, I_2 + IV, I_3 + V or I_2 + II + IV atoms (Fig. 1(a)). Most of MDLCs, including $CuInS_2$, Cu_2ZnSnS_4, etc., crystallize into chalcopyrite or stannite structure; however, the Cu_2SnS_3-type semiconductor takes a monoclinic structure with two types of anion-centered tetrahedra rather than one type of anion-centered tetrahedron in the whole structure.[14] As the substituting atoms own different ionic radii and electronegativities, the distorted lattice with diverse bonding length and angle will appear in MDLCs,[19,48,51,65] which can block the phonons from being transported and result in the relatively low κ. For example, the κ of $Cu_2ZnSnSe_4$ (Fig. 2(b)) is quite low in the whole temperature range, and it nearly decreases to 1.0 $W \cdot m^{-1} \cdot K^{-1}$ at high temperature, which is even comparable to the κ values of other TE materials with heavy constitute elements.[19,20] Meanwhile, the carrier mobility of MDLC will also decrease after substitution as compared with those of its binary counterparts.

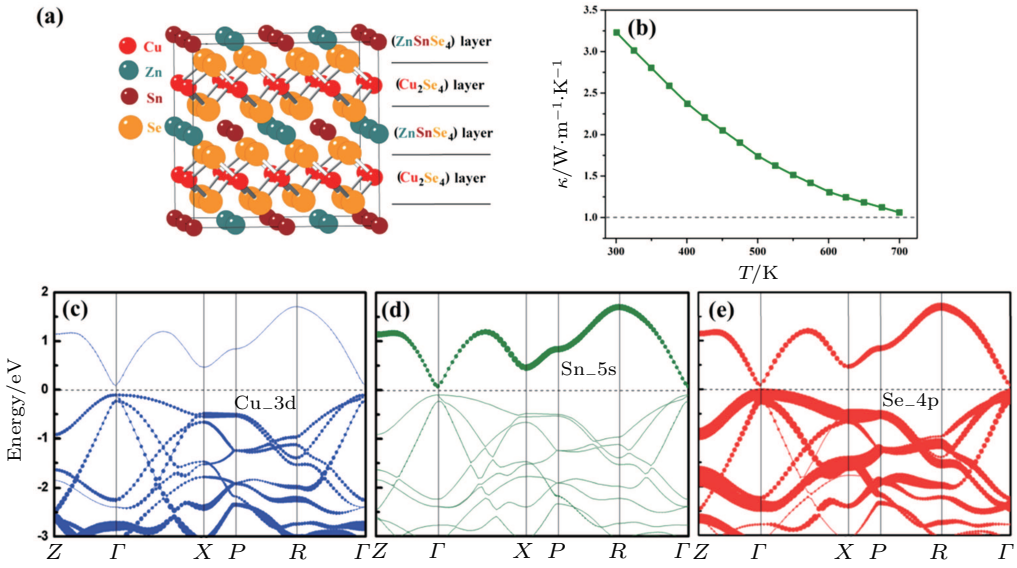


Fig. 2. (color online) (a) Structure of $Cu_2ZnSnSe_4$ with alternative (Cu_2Se_4) and ($ZnSnSe_4$) layers; (b) the temperature-dependent κ_L of $Cu_2ZnSnSe_4$;[20] [(c)–(e)] the orbital-decomposed band structures of $Cu_2ZnSnSe_4$.[73] Reproduced from Ref. [73] with permission from the Royal Society of Chemistry.

Owing to the similar characteristics in the crystalline structure, MDLCs have some similarities in electronic band structure. It should also be noted that the electronic structure for MDLCs was calculated very early,[68,69] and the results have become more and more accurate recently with the development of density functional theory.[70] For Cu-based ternary and quaternary chalcogenides, the valence band maximum (VBM) mainly contains a hybridization of Cu 3d orbitals and VI p orbitals because Cu has higher d orbital energy than the other cations, whereas the conduction band minimum (CBM) is primarily derived from the II/III/IV/V s orbital and VI p orbitals due to the lower s orbital energy of III/IV/V than the other cations.[14,70–72] For stannite $Cu_2ZnSnSe_4$ compound, the (Cu_2Se_4) tetrahedral slabs serve as the conduction pathway for holes and the insulating ($ZnSnSe_4$) ones can work as a charge reservoir (Fig. 2). One can also note that the valence band is relatively flat primarily due to the intrinsic localization of the Cu-3d electrons.[73] Moreover, the multiple bands at VBM can be utilized to yield a large Seebeck coefficient at high carrier concentration by band convergence, and result in the improved TE performance.[74]

3. Strategies to improve TE performance of MDLCs

3.1. Carrier concentration optimization

The intrinsic zT values for most of MDLCs are still very low primarily because their carrier concentrations are considerably lower than their corresponding optimal carrier concentrations, and thus resulting in the poor electrical transport properties. Thus, the common method of elemental doping is widely employed to increase carrier concentrations in MDLCs for achieving a high zT.[75] Importantly, the choice of doping site does lead to a difference in carrier mobility for heavily doped semiconductor, and high mobility is expected to be obtained when dopants are on the sub-lattice which makes less contributions to the formation of the charge-conducting band in principle, which is termed 'modulation doping on the atomic level (MDAL)' by Wang in the TE field.[76] High mobility is experimentally achieved from the anion-doped sample while the cation dopant is distinctly inferior in PbSe. We should point out that the enhanced mobility by this method can be observed when the band structure does not change (at least not significantly) with dopant. According to this concept, II/III/IV/V sites are reasonable doping places to increase the carrier concentration in p-type MDLC due to the above band structure features that the I–IV bonds dominate the p-type electrical transport while other elements (i.e., II/III/IV/V) exhibit weak contributions to the conductive framework. In experiment, substituting Sn with Indium was used as an effective guide to improve the carrier concentration in diamond-like Cu_2SnSe_3 compound and the generated hole would smoothly transport through three-dimensional (3D) Cu–Se conductive framework, thereby greatly enhancing the electrical properties.[48] Meanwhile, the copper deficiencies in Cu_2GeSe_3 are not effective in increasing the electrical properties.[77] Other investigations of Ge_{Sb}/Sn_{Sb} in Cu_3SbSe_4,[51,52,55–57] Zn_M in CuMTe$_2$ (M = Ga, In),[78–80] Cu_{Zn}/In_{Sn} in $Cu_2ZnSnSe_4$,[19,20] etc. also demonstrate the effectiveness of doping at II/III/IV/V sites in the enhancement of electrical properties and thus highly improving zTs. In addition, the possible presence of donor–acceptor defect pairs in MDLCs, such as ($V_{Cu}^{-} + Zn_{Cu}^{+}$) defect pairs in Cu_2ZnSnX_4 (X = S, Se),[81] will make the conducting mechanisms more complicated. For example, defect pairs (Zn_{Cu}^{+} and Zn_{In}^{-}) are introduced into zinc-doped $CuInTe_2$,[79] and the presence of antisite defect Zn_{Cu}^{+} defect will cancel the p-type carrier concentration and increase the ionized impurity scattering centers, which is harmful to the increase of electrical conductivity.

3.2. Band structure engineering

Previous studies indicated that the high band degeneracy (i.e., high N_v) and spin entropy are effective for decoupling the Seebeck coefficient and electrical conductivity, and thus improving the power factor significantly.[61,75] The above-mentioned approaches toward high zT in MDLCs will be discussed below.

3.2.1. Band convergence

(i) **Pseudocubic approach**

A high N_v number, which is normally observed in a crystal structure with high symmetry, is desired for gaining both a large Seebeck coefficient and high electrical conductivity. Snyder *et al.* successfully implemented the band-convergence scheme in Se-alloyed PbTe for the first time and attained an excellent zT value of ~ 1.8.[7] This scheme has also been successively applied in other highly symmetric semiconductors (e.g., Mg_2Si, SnTe, half–Heusler, and $CoSb_3$).[82–85] In 2014, Zhang *et al.* expanded it to chalcopyrite with low symmetry, and devised a 'pseudocubic approach' (Fig. 3), which has a cubic cation framework embedded in a noncubic distorted anion framework, to attain high power factor with high band convergence. They concluded a 'unity-η rule' ($\eta = c/2a$), which reveals that changing η toward unity would lead to band convergence for good thermoelectricity, and it was also experimentally verified that pseudocubic structured $CuInTe_2$ possesses the significantly enhanced zT value via Ag or Ga doping. As reported by Zeier *et al*. the pseudocubic approach truly works in attaining an increase of the power factor and zT in stannite $Cu_2ZnGeSe_4$ via Cu and Fe co-doping.[86] However, this promising approach is limited to low symmetry material with an ideal band gap and a low κ_L.[3]

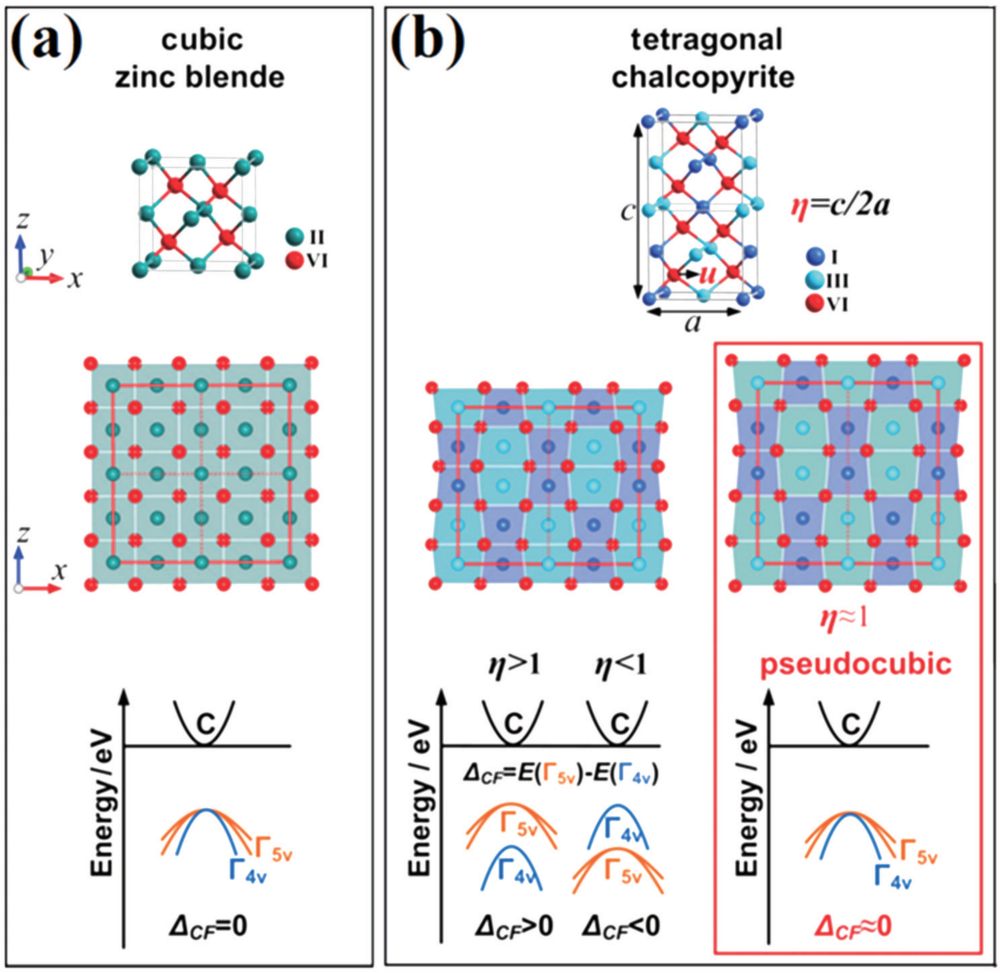


Fig. 3. (color online) Schematic diagrams illustrating the pseudocubic band-convergence, showing (a) crystal structure and schematic electronic bands of cubic zinc blende structure, and (b) crystal structure and schematic electronic bands of ternary chalcopyrites. The c and a are the lattice constants. Γ_{4v} is a nondegenerate band, and Γ_{5v} is a doubly degenerate band. Δ_{CF} is the crystal field-induced energy split at the top of the Γ_{4v} and Γ_{5v} bands. The pseudocubic structure has a cubic cation framework with Δ_{CF} embedded in a noncubic distorted anion framework.[23] Reproduced from Ref. [23] with permission from WILEY-VCH.

(ii) **Highly-efficient-doping (HED)**

As for TE materials possessing intrinsically high band degeneracy, heavy doping by guest atoms to reach the optimal carrier concentration will more or less cause the degenerate bands to destruct, leading to both the Seebeck coefficient and the power factor decreasing. Thus, selecting highly efficient dopants which can provide optimal carrier concentration at relatively low doping content, should be a feasible attempt to improve the electrical conductivity while maintaining the large Seebeck coefficient with little divergence of degenerate bands.[60] As illustrated in Fig. 4, the serious separation of the degenerate bands in non-HED can be relieved by HED when the same level of carrier concentration is reached. One could clearly note that the advantage of HED by Al/Ga/In comparing with the non-HED by Ge/Sn in high-band-degeneracy Cu_3SbSe_4 with 0.5% of Al/Ga/In substitution could provide comparable or even higher carrier concentration than that of 1% Ge-doping and its characteristic also has little deviation from the Pisarenko curve due to the nearly non-changed band structure. Meanwhile, the high doping concentration (e.g., 2% Ge, 5% Sn) makes the Seebeck coefficient deteriorate rapidly due to the severe split of the degenerate bands. Ultimately, the zT of the sample with HED possesses a higher value than that of the non-HED at 623 K.[60]

3.2.2. Spin entropy

It was suggested that the accompanying extra entropy in magnetic ions with degeneracy of electronic spin configuration in real space, such as transition metal ions with unpaired 3d electrons, should play a key role in obtaining large S at high σ in cobalt oxide.[61,87,88] This striking fact has encouraged many researchers to explore the possibility of substitution using magnetic ions to improve the TE performances of the other materials. Yao *et al*. firstly investigated the TE properties of magnetic-ion-substituted chalcopyrite in 2011 and observed the simultaneous optimizing of all three TE parameters in Mn-substituted $CuInSe_2$.[89] The Mn-doping moved the Fermi level (E_f) downward into the region of the valence band,

and the Mn 3d level hybridization with the Se 4p level resulted in the finite DOS in the proximity of the E_f, enabling the considerable enhancing of S and σ for $CuInSe_2$. The introduced Mn–Se networks could provide an additional conduction pathway for charge carriers. The increased local disorder in the crystal lattice by Mn substitution could reduce κ_L, which was also verified by Raman spectroscopy. However, the contribution of the spin entropy has been neglected in the work of Yao *et al*. In 2013, Xiao *et al.* reported that magnetic ions could also decouple the strongly interrelated three TE parameters in Cu_2ZnSnS_4 (Fig. 5(a)).[61] More importantly, the performed electron paramagnetic resonance (EPR) experiments implied that Ni^{2+} doping truly brought extra spin into Cu_2ZnSnS_4 and therefore the value of S is remarkably enhanced. After the magnetic ions (e.g., Cobalt) are fully substituted into Cu_2ZnSnS_4, the electronic structure and phonon structure will undergo significant change due to the strong hybridization between the 3d states of magnetic ions and S 3p states, and therefore the TE properties are improved (Figs. 5(b)–5(d)). The distinct band structure feature of Cu_2CoSnS_4 with magnetic component shows an extremely high zT of 0.8 achieved in this cheap and eco-friendly sulphide, which is due to the improved electrical properties by enhancing the effective mass and the depressed lattice thermal conductivity by weakening the covalent-bonding.[67]

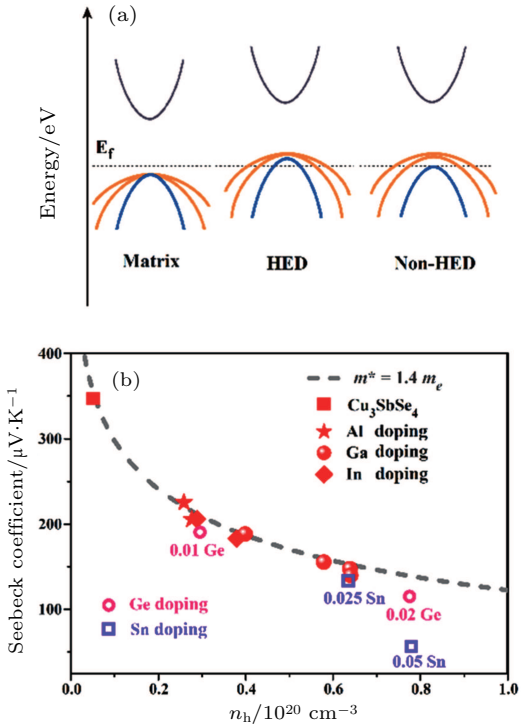


Fig. 4. (color online) (a) Schematic diagram illustrating the maintenance of highly degenerate electronic bands of the matrix by highly efficient doping (HED), and (b) curve of S versus carrier concentration showing that the nearly non-changed band structure can be obtained via HED (i.e., Al, Ga, In doping)[60] in Cu_3SbSe_4 with high band degeneracy. Reproduced from Ref. [6] with permission from the American Chemical Society.

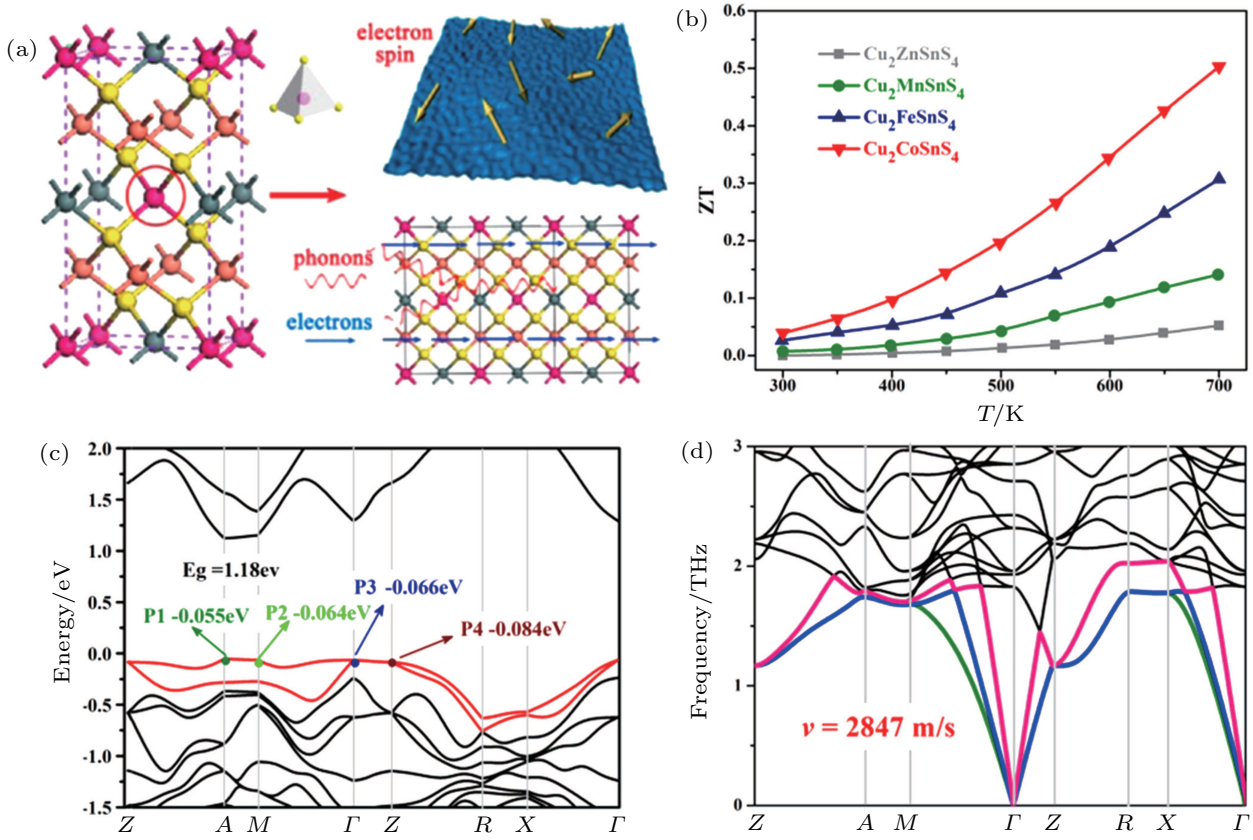


Fig. 5. (color online) (a) Schematic diagrams illustrating various electron spin and phonon scatterings in quaternary magnetic nanocrystals and (b) comparison of the zT among Cu_2XSnS_4 nanocrystals.[61] Reproduced from Ref. [61] with permission from the Royal Society of Chemistry, (c) electronic and (d) phonon band structure for Cu_2CoSnS_4.[67] Reproduced from Ref. [67] with permission from Elsevier.

Other researches for improving TE performances of Ni-doped Cu_3SbS_4, Mn-doped $CuGaTe_2$ and cobalt-doped Cu_2SnS_3,[46,90,91] also proved the effectiveness and good-transplanting of magnetic ion doping strategy in MDLCs. However, most of researches usually focused on explaining the enhancement in S by an additional spin entropy effect or the participation of magnetic-ion-3d states near the E_f in the electronic transport.[46,61,89–92] The above two factors, which may interconnect with each other by magnetic-ion, should be considered together and also clarify the primary cause for enhancing the value of S at different magnetic ion content (e.g., in 2.6% Ni-doped Cu_2ZnSnS_4, Cu_2CoSnS_4, and $CuFeS_2$).[36,61,67] Additionally, as the spin-disorder scattering in magnetic ion doping more or less hampers the mobility of carriers,[93] its influence should also be taken into consideration, especially at low temperature. If the reduction in carrier mobility overweighs the increase in S, no enhancement of power factor may appear. Therefore, the relationship between magnetism and TE property still needs further exploring.

3.3. Reduction of lattice thermal conductivity

3.3.1. Point-defect scattering

It is known that the introduction of point defects is an effective approach to reducing the value of κ_L by enhancing the phonon scattering due to the mass contrast and strain field fluctuation between the host and guest atoms. According to the Debye–Callaway–Klemens model, the high concentration of defects possessing large mass difference and strain fluctuations can maximize the scattering parameter (Γ) and thus achieve the lowest κ_L.[75] Pei *et al.* observed that Ag_{Cu} substitutional defects reduced the κ_L of $CuGaTe_2$ more obviously than Zn_{Ga}/In_{Ga} defects at the same concentration, which is due to the larger mass contrast.[94] However, the maximum mass contrast ($\Delta M/M = 1$), which can be maximized when the dominant point defects are vacancies, seems unattainable by conventional doping but is possible when the guest or host atom represents a disordered vacancy. Thus, the compounds with inherent vacancy, such as In_2Te_3 (one-third of its cationic sites are vacant) and their analogues, are selected to greatly depress the κ_L of the parent phase by forming a solid solution.[75] It is found that the value of κ_L of $CuGaTe_2$ alloyed with the proper amount of In_2Te_3 or Ga_2Te_3 was reduced more remarkably than that of the same quantity of substitutional defects (Fig. 6(a)), which could be attributed to the strong vacancy phonon scattering induced by guesting vacancies.[95] Additionally, a detailed investigation of the room temperature thermal conductivity on anion substitution series $Cu_2ZnGeSe_{4-x}S_x$ revealed a reduction of the κ_L of 42% (Fig. 6(b)), and the calculations quantitively revealed that mass contrast (reduction of 34%) has a greater influence than strain contrast (reduction of 8%).[96]

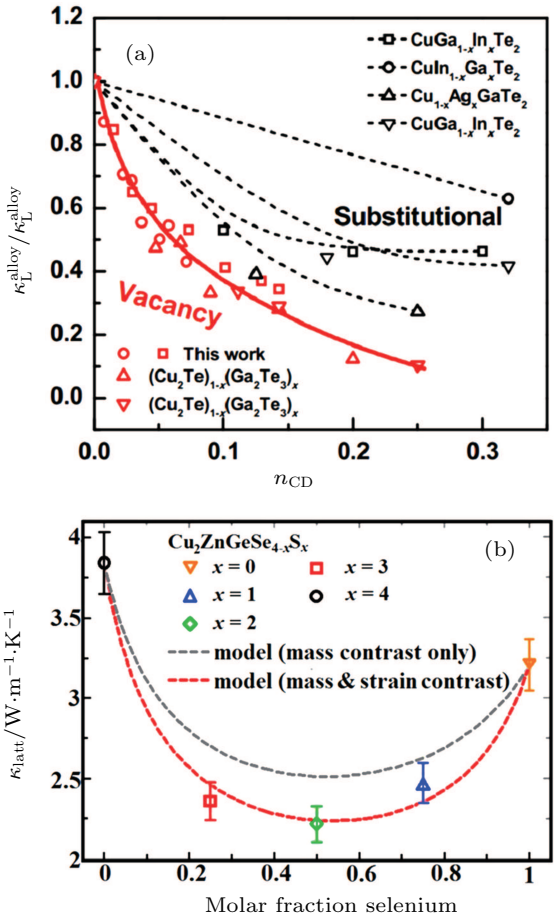


Fig. 6. (color online) (a) Room temperature cation defect concentration (n_{CD})-dependent normalized lattice thermal conductivity (κ_L) for $CuGaTe_2$ solid solutions with (red) and without (black) vacancies.[95] Reproduced from Ref. [95] with permission from the Royal Society of Chemistry. (b) Plots of room-temperature κ_L and modeled κ_L against the molar fraction of selenium of the complete solid solution series $Cu_2ZnGeSe_{4-x}S_x$ with $x = 0$–4.[96] Reproduced from Ref. [96] with permission from the American Chemical Society.

3.3.2. Nanostructure engineering

(I) **Nanocomposite**

The proposed concept of low-dimensional TE materials (e.g. quantum dots, nanowires and superlattices systems) in the 1990s has revealed that the simultaneous optimization of the power factor and κ_L is possible in nanostructures.[97,98] After that, many experimental studies on nanostructured bulk materials, such as $(Bi,Sb)_2Te_3$, PbTe, $Si_{80}Ge_{20}$,[99–101] have also proved that the nanocomposite approach (i.e., reducing the grain size to nanometers or using nanoparticles) is indeed effective in increasing zT of 3D bulk material due to the reduction in the κ_L by the selective scattering of phonons or the enhancement in the Seebeck coefficient via preferential scattering of low-energy electrons (i.e., energy filtering).[12] Consequently, the nanocomposite approach is also widely adopted to achieve the expected high zT in MDLC, although it probably causes the electrical conductivity to decrease by the deterioration of carrier mobility. Liu *et al.* reported a solution-based scalable synthesis approach to produce several grams of monodisperse Cu_3SbSe_4 nanocrystals (Fig. 7),[59] and found the nano-crystalline Cu_3SbSe_4 had better TE per-

formance than the micro-crystalline compound with the same constituents because the value of κ_L greatly decreased. Furthermore, an extremely high zT value (i.e., 1.26) was obtained in (Sn, Bi)-dual-doped Cu_3SbSe_4 by this improved approach. Liang *et al*. found that the $CuFeS_2$ nanocrystals exhibited a significantly higher S than bulk chalcopyrite material due to quantum confinement and a tremendously low κ_L, due to the increased phonon scattering at the nanocrystal grain boundary, thus zT is enhanced by 77 times.[36] Chen *et al*. found that Cu-doped $Cu_2ZnSnSe_4$ nanocrystals prepared by hot-injection had a zT as high as 0.70 at 450 °C, which is significantly higher than that by the traditional method.[63] The obtained high TE performance in Cu_2SnSe_3 nanocrystal also shows the effectiveness and good prospects of the nanocomposite approach in obtaining efficient TE materials.[13] However, the problems of aggregation and growth during nanocrystals densification become challenges to further enhancing the TE performance by this approach.

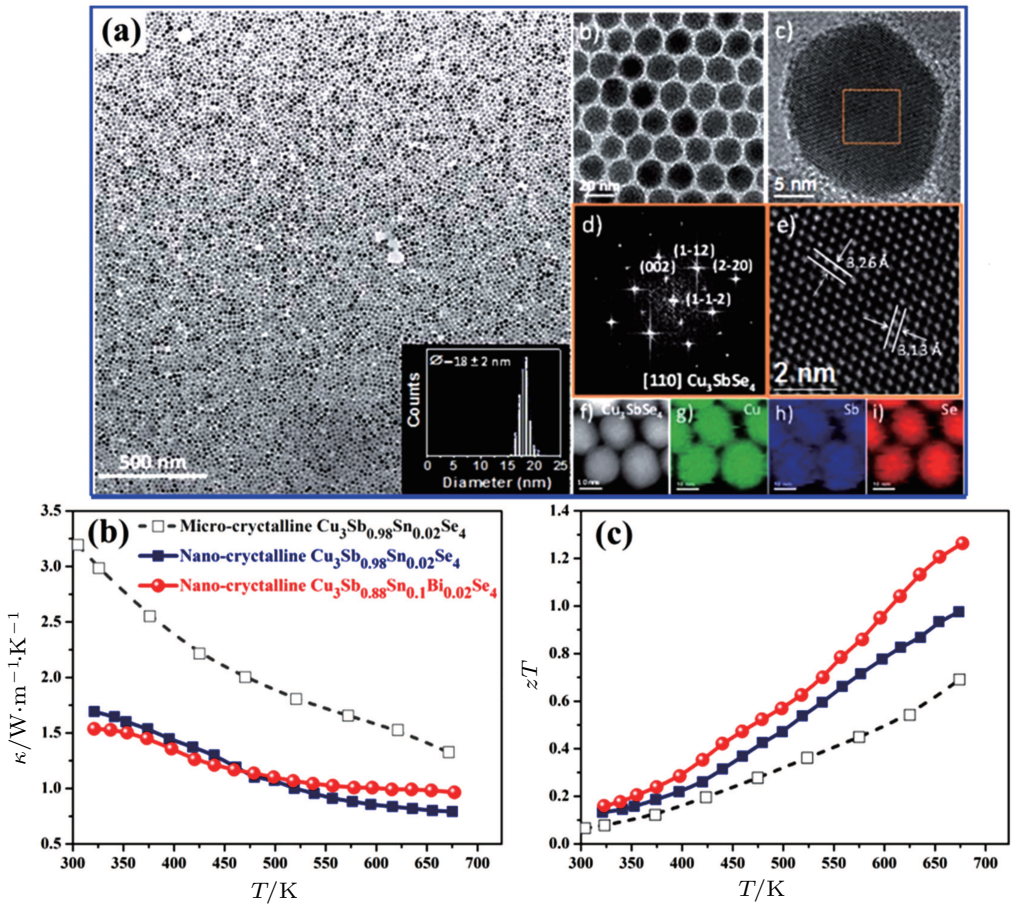


Fig. 7. (color online) (a) Representative TEM micrographs of Cu_3SbSe_4 nanocrystallines, and the corresponding HRTEM images, electron diffraction patterns and EELS analysis results.[59] Reproduced from Ref. [59] with permission from the Royal Society of Chemistry. [(b) and (c)] Temperature-dependent κ and zT values for micro- and nano-crystalline Cu_3SbSe_4.[56,59]

(II) **Nanoinclusion**

Nanoinclusion strategies by introducing a nano-sized second phase are effectively utilized to obtain high performance TE materials (e.g., $CoSb_3$, PbTe, SnTe)[104–106] due to the depressed κ_L by additional phonon scattering or the increased S through energy filtering. Most of the research of nanoinclusion about MDLCs focuses on the $CuGaTe_2$/$CuInTe_2$ type materials currently. In the case of $CuGaTe_2$, the incorporation of graphite nanosheets could enhance the S and power factor due to the energy filtering effect, and also cause the value of κ_L to decrease below 750 K because of the increased interface scattering. The large zT value increased up to 0.93 at 873 K in $CuGaTe_2$ composite, which had about 21% improvement on pure $CuGaTe_2$.[107] However, the introduction of nanophase Cu_2Se into $CuGaTe_2$ reduced the value of S due to the increase of carrier concentration.[32] Benefiting from the greatly reduced value of κ_L, the final zT approached to 1.2 at 834 K for the $CuGaTe_2$/3vol% Cu_2Se sample. By introducing a proper amount of grapheme into $CuInTe_2$, Chen *et al*. also observed that the κ_L successfully decreased and also the value of zT was improved.[108]

4. Synergistic regulation

4.1. Entropy engineering

Recently, high entropy alloy (HEA), which consists of multiple principal elements in an equimolar manner or in a close to equimolar ratio manner, has been proposed as a

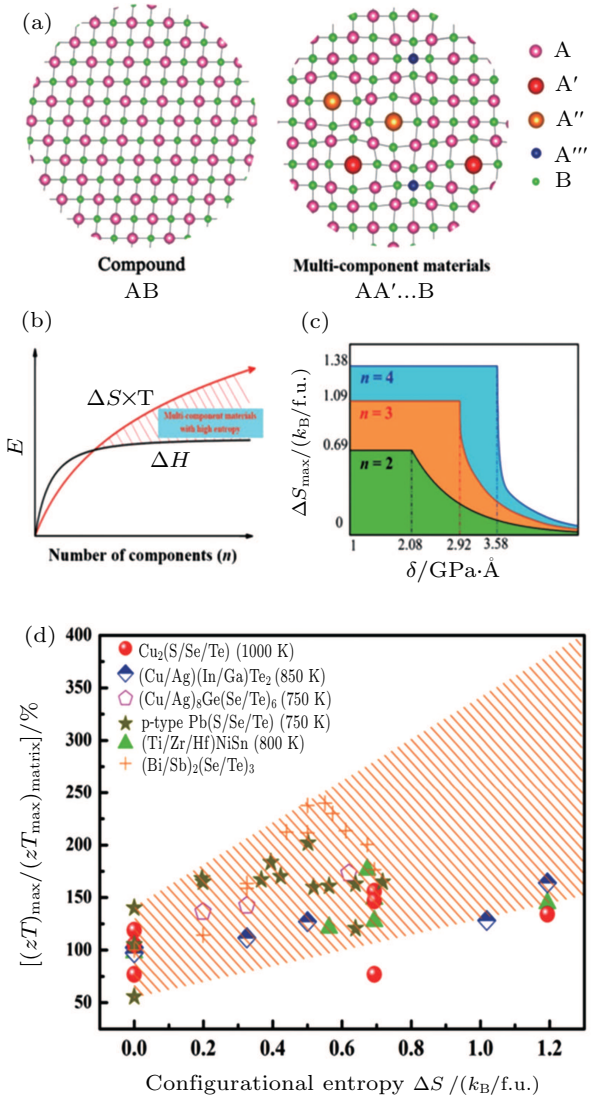


Fig. 8. (color online) (a) Schematic diagrams of the lattice framework in multicomponent materials compared with an ordinary binary compound. (b) Schematic diagram of the entropy engineering with multicomponent TE materials. (c) Maximum confgurational entropy (in units of k_B per formula unit) as a function of material solubility parameter δ for given multicomponent TE materials, where n is the number of components. (d) Plots of maximum zT versus confgurational entropy in $Cu_2(S/Se/Te)$-, $(Cu/Ag)(In/Ga)Te_2$-, and $Cu_8Ge(Se/Te)_6$-based multicomponent TE materials.[26] Reproduced from Ref. [26] with permission from WILEY-VCH.

novel type of alloy with intriguing properties in structure and function.[109,110] Due to the chemical complexity (e.g., large atomic size differences) and high configuration entropy, HEA may significantly introduce extra phonon scattering and also offer a new way to adjust electrons, and resultantly affect the electrical and thermal properties. The HEA was introduced into the context of TE by Shafeie *et al*. as a potential candidate for future TE material.[111] In this scenario, Liu *et al*. devised a strategy of using entropy as the global genelike performance indicator, which shows how multicomponent thermoelectric materials with high entropy could be designed (Fig. 8).[29] They first defined a parameter δ in a novel elastic model by shear modulus, lattice parameter and the mismatch in the atomic radius as a criterion for judging the feasibility of forming a complete solid solution with high entropy. Guided by the δ criterion, they screened out several multicomponent TE material systems. Finally, the screened candidates were experimentally tested and the enhanced zT values approached to 1.6 and 2.23 in respective $(Cu/Ag)(In/Ga)Te_2$- and $Cu_2(S/Se/Te)$-based multicomponent materials due to the optimization of entropy. Hence, entropy engineering using multicomponent crystal structures works as an effective guide to greatly improve the TE performance through the simultaneous optimization of electrical and thermal transport properties, i.e., to lower κ_L by the presence of local mass and strain fluctuations and to improve the S by enhancing the crystal symmetry. Lu *et al*. also observed that PbSnTeSe HEAs possess quite low κ_L, for example, less than 0.6 $W\cdot m^{-1}\cdot K^{-1}$ at 300 K, and its TE properties could be further enhanced by slight composition alteration.[112] Although this strategy holds promise for reducing the value of κ_L, the simultaneously observed improvement of S is limited to some TE materials with increased crystal symmetry.

4.2. *In-situ* displacement reaction

Nano-oxide additives are commonly used to reduce κ_L by introducing additional phonon scattering into TE materials, and the oxides are usually stable in the host material because of their intrinsically strong bonding.[113–119] In 2016, Luo *et al*. first discovered the *in-situ* displacement reaction between the ZnO additive and the $CuInTe_2$ matrix at 714 K by differential scanning calorimeter (DSC) and transmission electron microscopy (TEM) as displayed in Figs. 9(a)–9(c),[26] and this reaction is partially understandable in the bonding strength respect: the final product of In_2O_3 possessing stronger bonds is more stable than ZnO due to the higher melting point (T_m of $In_2O_3 \sim 2273$ K and T_m of ZnO ~ 2248 K). Thus, it has two significant effects on tuning and optimizing electrical and thermal transport properties, i.e., to lower the thermal conductivity via the extra phonon scattering from In_2O_3 nanoinclusions, and to improve the electrical conductivity by the formation of Zn_{In}^{-} point defects. Then, an 80% enhanced zT value of 1.44 was obtained in the 1-wt% ZnO added $CuInTe_2$ sample. Moreover, by integrating the anion substitution (i.e., Sb doping) and *in-situ* displacement reaction, a high power factor of 1445 $\mu W\cdot m^{-1}\cdot K^{-2}$ and unprecedented zT of 1.61 at 823 K were achieved in the $CuInTe_2$ based TE material (Fig. 10(d)). In addition, the simultaneous regulation of electrical and thermal transport properties in TiO_2 added $CuInTe_2$ also proved the effectiveness of *in-situ* displacement reaction by other oxides in improving TE performance.[25]

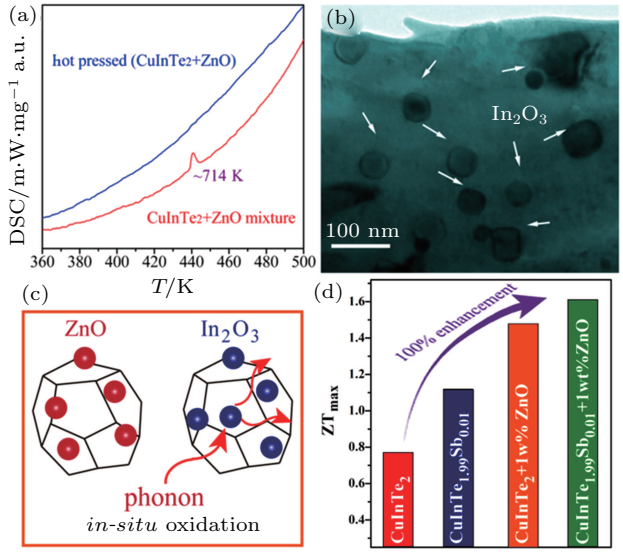


Fig. 9. (color online) (a) DSC curves of $CuInTe_2 + 2.0$-wt% ZnO additives before and after hot press process. (b) Highly magnified TEM images of $CuInTe_2$ matrix with dispersed In_2O_3 nanoparticles. Reproduced from Ref. [25] with permission from Elsevier. (c) Scheme of *in-situ* displacement reaction. (d) Stepping increase of zT at 823 K in the $CuInTe_2$ samples by Sb substitution, ZnO adding, and combined Sb substitution, and ZnO adding.[25,26] Reproduced from Ref. [26] with permission from WILEY-VCH.

5. TE devices

Since research on the TE properties of MDLCs is still in the early stage, most of the attention is paid to enhancing the zTs and the feasibility to fabricate an efficient TE device based on MDLCs is still an open question. In 2017, researchers started to address this inevitable question

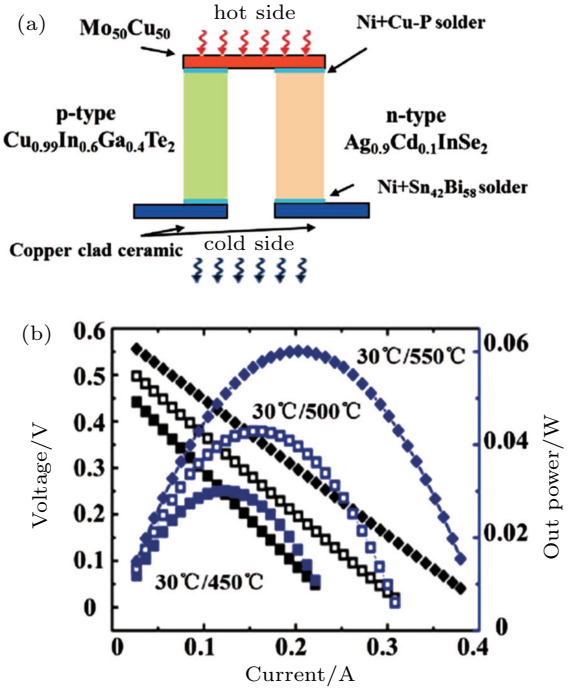


Fig. 10. (color online) (a) Schematic diagram of the structure of the fabricated diamond-like module, and b) plots of output voltage (black) and power (blue) versus current for TE module based on diamond-like materials. Temperature differences between the cold side and the hot side of the module are 420, 470, and 520 K, respectively.[35]

and finally opened the door for practical applications of MDLCs TE materials. Due to the obtained high TE performance in (Sn, Bi)-codoped nanocrystalline Cu_3SbSe_4 sample, Liu *et al.* used them to fabricate an innovative ring-shaped TE generator with a single p-leg, which could be used to recover the waste heat from exhaust gas pipes of vehicles.[59] The results showed that an open circuit voltage near 20 mV was obtained for a single TE element when the temperature gradient was maintained at 160 K. Then, the first TE module including both n and p-type MDLCs was fabricated by Qiu *et al.* as shown in Fig. 10.[35] The TE module using $Ag_{0.9}Cd_{0.1}InSe_2$ and $Cu_{0.99}In_{0.6}Ga_{0.4}Te_2$ as respective n- and p-type legs presented a maximum output power of 0.06 W under a temperature difference of 520 K, clearly showing that MDLCs can be a potential candidate for TE applications.

6. Conclusions and perspectives

In this review, we mainly discuss the features in crystal structure and electronic structure, and summarize the effective strategies to enhance zTs for MDLCs. Due to the unique diamond-structure-accompanied properties: flat valence band and large local distortion, MDLCs usually possess both relatively high Seebeck coefficients and low thermal conductivities. A zT value as high as 1.6 is achieved in Pb-free MDLC by entropy engineering or by *in-situ* displacement reaction, thus highlighting the promising prospect of MDLCs for TE applications. However, more efforts are still needed to promote the practical TE applications of MDLCs. On the one hand, the zT value especially the average one cannot be so good as that of highly efficient PbTe-based TE material, so it is of great importance to further increase the zTs by new strategies.[9,120–122] Recently, it was demonstrated that dislocation arrays, which effectively scatter phonons and maintain high carrier mobility could concurrently optimize the electrical and thermal transport properties, leading to a great improvement of both power factor and zT in $CoSb_3$- or $(Bi,Sb)_2Te_3$-based TE materials.[123,124] Pei *et al.* also noted that the dense in-grain dislocations indeed took the major responsibility for the decrease of κ_L through scattering the remaining mid-frequency phonons thereby resulting in the extremely low κ_L approaching to the amorphous limit.[125] Hence, dislocation engineering is a good direction for further obtaining advanced MDLC TE materials. Besides, the resonant levels play an important role in enhancing both the average power factor and zT value in SnTe, which is mainly due to the increased S.[126,127] Nanoheterostructure-based nanocomposites (e.g., PbTe–Ag_2Te, PbTe–BiSbTe) present both the improved power factor and the depressed κ_L because of minority carrier blocking.[128,129] Can the resonant levels also increase S or does the nanoheterostructure block the minority carrier in MDLC?

The poor TE properties in n-type MDLCs also hamper the TE applications of this promising typed material, because

a TE device requires both a high-performance n-type leg and a high-performance p-type leg. In the literature, the highest zT in reported n-type MDLCs is still inferior to that of the p-type one, such as 0.126 at 450 K for $CuFeInTe_3$,[130] 0.264 at 500 K for $CuFeS_2$, and 1.1 at 900 K for $AgInSe_2$.[35,36] Meanwhile, it seems difficult to change the intrinsic p-type conduction into an n-type one for most of MDLCs with high TE performance. For instance, zinc-doping heavily at the copper site could not make the n-type Cu_3SbSe_4 available.[131] The origin of p-type electrical transports in most of MDLCs might be linked to the presence of intrinsic Cu vacancies.[132] Thus, discovering and realizing n-type MDLCs with high TE performance is urgently needed in the future research. In addition, the stability investigation of MDLCs under thermal cycling or large current, which is of great importance in practical applications, should also be focused on.[133]

References

[1] Bell L E 2008 *Science* **321** 1457
[2] DiSalvo F J 1999 *Science* **285** 703
[3] He J and Tritt T M 2017 *Science* **357** eaak9997
[4] Shuai J, Mao J, Song S, Zhang Q, Chen G and Ren Z 2017 *Mater. Today Phys.* **1** 74
[5] Xiao C, Li Z, Li K, Huang P and Xie Y 2014 *Acc. Chem. Res.* **47** 1287
[6] Heremans J P, Jovovic V, Toberer E S, Saramat A, Kurosaki K, Charoenphakdee A, Yamanaka S and Snyder G J 2008 *Science* **321** 554
[7] Pei Y, Shi X, LaLonde A, Wang H, Chen L and Snyder G J 2011 *Nature* **473** 66
[8] Shi X, Yang J, Salvador J R, Chi M, Cho J Y, Wang H, Bai S, Yang J, Zhang W and Chen L 2011 *J. Am. Chem. Soc.* **133** 7837
[9] Biswas K, He J, Blum I D, Wu C I, Hogan T P, Seidman D N, Vinayak P D and Kanatzidis M G 2012 *Nature* **489** 414
[10] Zhao W, Liu Z, Sun Z, Zhang Q, Wei P, Mu X, Zhou H, Li C, Ma S, He D, Ji P, Zhu W, Nie X, Su X, Tang X, Shen B, Dong X, Yang J, Liu Y and Shi J 2017 *Nature* **549** 247
[11] Qiu P, Shi X and Chen L 2016 *Energy Storage Materials* **3** 85
[12] Zhang D, Yang J, Jiang Q, Fu L, Xiao Y, Luo Y and Zhou Z 2016 *J. Mater. Chem. A* **4** 4188
[13] Zhang D, Yang J, Jiang Q, Fu L, Xiao Y, Luo Y and Zhou Z 2016 *Mater. Des.* **98** 150
[14] Xi L, Zhang Y B, Shi X Y, Yang J, Shi X, Chen L D and Zhang W 2012 *Phys. Rev. B* **86** 155201
[15] Contreras M A, Egaas B, Ramanathan K, Hiltner J, Swartzlander A, Hasoon F and Noufi R 1999 *Prog. Photovoltaics Res. Appl.* **7** 311
[16] Mousa N H, El-bahay M M, Abdelghany A and Abou El Ela A H 1996 *Phys. Chem. Liq.* **33** 113
[17] Kuhn B, Kaefer W, Fess K, Friemelt K, Turner C, Wendl M and Bucher E 1997 *Phys. Stat. Sol. A* **162** 661
[18] Endo S, Sudo I and Irie T 1971 *Jpn. J. Appl. Phys.* **10** 218
[19] Liu M L, Huang F Q, Chen L D and Chen I W 2009 *Appl. Phys. Lett.* **94** 202103
[20] Shi X Y, Huang F Q, Liu M L and Chen L D 2009 *Appl. Phys. Lett.* **94** 122103
[21] Liu R, Xi L, Liu H, Shi X, Zhang W and Chen L 2012 *Chem. Commun.* **48** 3818
[22] Li Y, Meng Q, Deng Y, Zhou H, Gao Y, Li Y, Yang J and Cui J 2012 *Appl. Phys. Lett.* **100** 231903
[23] Zhang J, Liu R, Cheng N, Zhang Y, Yang J, Uher C, Shi X, Chen L and Zhang W 2014 *Adv. Mater.* **26** 3848
[24] Carr W D and Morelli D T 2015 *J. Alloys Compd.* **630** 277
[25] Luo Y, Yang J, Jiang Q, Li W, Xiao Y, Fu L, Zhang D, Zhou Z and Cheng Y 2015 *Nano Energy* **18** 37
[26] Luo Y, Yang J, Jiang Q, Li W, Zhang D, Zhou Z, Cheng Y, Ren Y and He X 2016 *Adv. Energy Mater.* **6** 1600007
[27] Liu R, Qin Y, Cheng N, Zhang J, Shi X, Grin Y and Chen L 2016 *Inorg. Chem. Front.* **3** 1167
[28] Luo Y, Jiang Q, Yang J, Li W, Zhang D, Zhou Z, Cheng Y, Ren Y, He X and Li X 2017 *Nano Energy* **32** 80
[29] Liu, R, Chen H, Zhao K, Qin Y, Jiang B, Zhang T, Sha G, Shi X, Uher C, Zhang W and Chen L 2017 *Adv. Mater.* **29** 1702712
[30] Plirdpring T, Kurosaki K, Kosuga A, Day T, Firdosy S, Ravi V, Snyder J F, Harnwunggmoung A, Sugahara T, Ohishi Y, Muta H and Yamanaka S 2012 *Adv. Mater.* **24** 3622
[31] Cui J, Li Y, Du Z, Meng Q and Zhou H 2013 *J. Mater. Chem. A* **1** 677
[32] Zhang J, Qin X, Li D, Xin H, Song C, Li L, Zhu X, Wang Z, Guo G and Wang L 2014 *J. Mater. Chem. A* **2** 2891
[33] Yusufu A, Kurosaki K, Kosuga A, Sugahara T, Ohishi Y, Muta H and Yamanaka S 2011 *Appl. Phys. Lett.* **99** 061902
[34] Ying P Z, Zhou H, Gao Y L, Li Y Y, Li Y P, Lian X L and Cui J L 2012 *Key Eng. Mate.* **519** 188
[35] Qiu P, Qin Y, Zhang Q, Li R, Yang J, Song Q, Tang Y, Bai S, Shi X and Chen L 2017 *Adv. Sci.* **4** 1700727
[36] Liang D, Ma R, Jiao S, Pang G and Feng S 2012 *Nanoscale* **4** 6265
[37] Tsujii N and Mori T 2013 *Appl. Phys. Express* **6** 043001
[38] Li J, Tan Q and Li J F 2013 *J. Alloys Compd.* **551** 143
[39] Li Y, Zhang T, Qin Y, Day T, Jeffrey S G, Shi X and Chen L 2014 *J. Appl. Phys.* **116** 203705
[40] Berthebaud D, Lebedev O I and Maignan A 2015 *J. Materiomics* **1** 68
[41] Carr W D and Morelli D T 2016 *J. Electronic Mater.* **45** 1346
[42] Lefèvre R, Berthebaud D, Mychinko M Y, Lebedev O I, Mori T, Gascoin F and Maignan A 2016 *RSC Adv.* **6** 55117
[43] Xie H, Su X, Zheng G, Zhu T, Yin K, Yan Y, Uher C, Kanatzidis M G and Tang X 2017 *Adv. Energy Mater.* **7** 1601299
[44] Xie H, Su X, Yan Y, Liu W, Chen L, Fu J, Yang Y, Uher C and Tang X 2017 *NPG Asia Mater.* **9** e390
[45] Tan Q, Sun W, Li Z and Li J F 2016 *J. Alloys Compd.* **672** 558
[46] Zhao H, Xu X, Li C, Zhang R, Huang R, Lv Y, Li D, Hu X, Pan L and Wang Y 2017 *J. Mater. Chem. A* **5** 23267
[47] Cho J Y, Shi X, Salvador J R, Meisner G P, Yang J, Wang H, Wereszczak A A, Zhou X and Uher C 2011 *Phys. Rev. B* **84** 085207
[48] Shi X, Xi L, Fan J, Zhang W, Chen L 2010 *Chem. Mater.* **22** 6029
[49] Li, Y, Liu G, Cao T, Liu L, Li J, Chen K, Li L, Han Y and Zhou M 2016 *Adv. Funct. Mater.* **26** 6025
[50] Chen K, Du B, Bonini N, Weber C, Yan H, and Reece M J 2016 *J. Phys. Chem. C* **120** 27135
[51] Yang C, Huang F, Wu L and Xu K 2011 *J. Phy. D: Appl. Phys.* **44** 295404
[52] Skoug E J, Cain J D and Morelli D T 2011 *Appl. Phys. Lett.* **98** 261911
[53] Li X Y, Li D, Xin H X, Zhang J, Song C J and Qin X Y 2013 *J. Alloys Compd.* **561** 105
[54] Li D, Li R, Qin X Y, Zhang J, Song C J, Wang L and Xin X 2013 *CrystEngComm* **15** 7166
[55] Li D, Li R, Qin X Y, Song C J, Xin H X, Wang L, Zhang J, Guo G L, Zou T H, Liu Y F and Zhu X G 2014 *Dalton Trans.* **43** 1888
[56] Wei T R, Wang H, Gibbs Z M, Wu C F, Snyder G J and Li J F 2014 *J. Mater. Chem. A* **2** 13527
[57] Chang C H, Chen C L, Chiu W T and Chen Y Y 2017 *Mater. Lett.* **186** 227
[58] Zhang D, Yang J, Jiang Q, Zhou Z, Li X, Ren Y, Xin J, Basit A, He X, Chu W and Hou J 2017 *J. Alloys Compd.* **724** 597
[59] Liu Y, García G, Ortega S, Cadavid D, Palacios P, Lu J, Ibáñez M, Xi L, Roo J D, López A M, Martí-Sánchez S, Cabezas I, Mata M, Luo Z, Dun C, Dobrozhan O, Carroll D L, Zhang W, Martins J, Kovalenko M V, Arbiol J, Noriega G, Song J, Wahnón P and Cabot A 2017 *J. Mater. Chem. A* **5** 2592
[60] Zhang D, Yang J, Jiang Q, Zhou Z, Li X, Xin J, Basit A, Ren Y, He X, Chu W and Hou J 2017 *ACS Appl. Mater. Interfaces* **9** 28558
[61] Xiao C, Li K, Zhang J, Tong W, Liu Y, Li Z, Huang P, Pan B, Su H and Xie Y 2014 *Mater. Horiz.* **1** 81
[62] Dong Y, Wang H, Nolas G S 2014 *Phys. Status Solidi-RRL* **8** 61
[63] Chen D, Zhao Y, Chen Y, Wang Y, Zhou J and Liang Z 2015 *ACS Appl. Mater. Interfaces* **7** 24403
[64] Zeier W G, LaLonde A, Gibbs Z M, Heinrich C P, Panthöfer M, Snyder G J and Tremel W 2012 *J. Am. Chem. Soc.* **134** 7147
[65] Liu M L, Chen I W, Huang F Q and Chen L D 2009 *Adv. Mater.* **21** 3808
[66] Song Q, Qiu P, Hao F, Zhao K, Zhang T, Ren D, Shi X and Chen L 2016 *Adv. Electron. Mater.* **2** 1600312

[67] Zhang D, Yang J, Jiang Q, Zhou Z, Li X, Xin J, Basit A, Ren Y and He X 2017 *Nano Energy* **36** 156

[68] Jaffe J E and Zunger A 1983 *Phys. Rev. B* **28** 5822

[69] Jaffe J E and Zunger A 1984 *Phys. Rev. B* **29** 1882

[70] Zhang Y, Xi L, Wang Y, Zhang J, Zhang P and Zhang W 2015 *Comp. Mater. Sci.* **108** 239

[71] Chen S, Gong X G, Walsh A and Wei S H 2009 *Appl. Phys. Lett.* **94** 041903

[72] Zhang Y, Zhang J, Gao W, Abtew T A, Wang Y, Zhang P and Zhang W 2013 *J. Chem. Phys.* **139** 184706

[73] Zou D, Nie G, Li Y, Xu Y, Lin J, Zheng H and Li J 2015 *RSC Adv.* **5** 24908

[74] Zhao L D, Tan G, Hao S, He J, Pei Y, Chi H, Wang H, Gong S, Xu H, Dravid V P, Uher C, Snyder G J, Wolverton C and Kanatzidis M G 2016 *Science* **351** 141

[75] Tan G, Zhao L D and Kanatzidis M G 2016 *Chem. Rev.* **116** 12123

[76] Wang H, Cao X, Takagiwa Y and Snyder G J 2015 *Mater. Horiz.* **2** 323

[77] Huang T, Yan Y, Peng K, Tang X, Guo L, Wang R, Lu X, Zhou X and Wang G 2017 *J. Alloys Compd.* **723** 708

[78] Luo P, You L, Yang J, Xing J, Zhang J, Wang C, Zhao X, Luo J and Zhang W 2017 *Chin. Phys. B* **26** 097201

[79] Yang J, Chen S, Du Z, Liu X and Cui J 2014 *Dalton Trans.* **43** 15228

[80] Shen J, Chen Z, Lin S, Zheng L, Li W and Pei Y 2016 *J. Mater. Chem. C* **4** 209

[81] Chen S, Yang J H, Gong X G, Walsh A and Wei S H 2010 *Phys. Rev. B* **81** 245204

[82] Liu W, Tan X, Yin K, Liu H, Tang X, Shi J, Zhang Q and Uher C 2012 *Phys. Rev. Lett.* **108** 166601

[83] Fu C, Zhu T, Pei Y, Xie H, Wang H, Snyder G J, Liu Y, Liu Y and and Zhao X 2014 *Adv. Energy Mater.* **4** 1400600

[84] Tang Y, Gibbs Z M, Agapito L A, Li G, Kim H S, Nardelli M B, Curtarolo S and Snyder G J 2015 *Nat. Mater.* **14** 1223

[85] Banik A, Shenoy U S, Anand S, Waghmare U V and Biswas K 2015 *Chem. Mater.* **27** 581

[86] Zeier W G, Zhu H, Gibbs Z M, Ceder G, Tremel W and Snyder G J 2014 *J. Mater. Chem. C* **2** 10189

[87] Wang Y, Rogado N S, Cava R J and Ong N P 2003 *Nature* **423** 425

[88] Limelette P, Hébert S, Hardy V, Frésard R, Simon C and Maignan A 2006 *Phys. Rev. Lett.* **97** 046601

[89] Yao J, Takas N J, Schliefert M L, Paprocki D S, Blanchard P E, Gou H, Mar A, Exstrom C L, Darveau S A, Poudeu P F P and Aitken J A 2011 *Phys. Rev. B* **84** 075203

[90] Chen D, Zhao Y, Chen Y, Lu T, Wang Y, Zhou J and Liang Z 2016 *Adv. Electron. Mater.* **2** 1500473

[91] Ahmed F, Tsujii N and Mori T 2017 *J. Mater. Chem. A* **5** 7545

[92] Mori T 2017 *Small* **13** 1702013

[93] Brown S R, Toberer E S, Ikeda T, Cox C A, Gascoin F, Kauzlarich S M and Snyder G J 2008 *Chem. Mater.* **20** 3412

[94] Shen J, Zhang X, Chen Z, Lin S, Li J, Li W, Li S, Chen Y and Pei Y 2017 *J. Mater. Chem. A* **5** 5314

[95] Shen J, Zhang X, Lin S, Li J, Chen Z, Li W and Pei Y 2016 *J. Mater. Chem. A* **4** 15464

[96] Heinrich C P, Day T W, Zeier W G, Snyder G J and Tremel W 2014 *J. Am. Chem. Soc.* **136** 442

[97] Hicks L D and Dresselhaus M S 1993 *Phys. Rev. B* **47** 12727

[98] Dresselhaus M S, Chen G, Tang M Y, Yang R G, Lee H, Wang D Z, Ren Z F, Fleurial J P and Gogna P 2007 *Adv. Mater.* **19** 1043

[99] Poudel B, Hao Q, Ma Y, Lan Y, Minnich A, Yu B, Yan X, Wang D, Muto A, Vashaee D and Chen X 2008 *Science* **320** 634

[100] Finefrock S W, Zhang G, Bahk J H, Fang H, Yang H, Shakouri A and Wu Y 2014 *Nano Lett.* **14** 3466

[101] Joshi G, Yan X, Wang H, Liu W, Chen G and Ren Z 2011 *Adv. Energy Mater.* **1** 643

[102] Jiang Q, Yang J, Liu Y and He H 2016 *J. Adv. Dielectr.* **6** 1630002

[103] Ibáñez M, Cadavid D, Anselmi-Tamburini U, Zamani R, Gorsse S, Li W, López A M, Morante J R, Arbiol J and Cabot A 2013 *J. Mater. Chem. A* **1** 1421

[104] Peng J, Fu L, Liu Q, Liu M, Yang J, Hitchcock D, Zhou M and He J 2014 *J. Mater. Chem. A* **2** 73

[105] Biswas K, He J, Blum I D, Wu C I, Hogan T P, Seidman D N, Dravid V P and Kanatzidis M G 2012 *Nature* **489** 414

[106] Moshwan R, Yang L, Zou J and Chen Z G 2017 *Adv. Funct. Mater.* **27** 1703278

[107] Zhang J, Qin X, Li D, Liu Y, Li Y, Song C Xin H and Zhu X 2016 *Appl. Phys. Lett.* **108** 073902

[108] Chen H, Yang C, Liu H, Zhang G, Wan D and Huang F 2013 *CrystEngComm* **15** 6648

[109] Li Z, Pradeep K G, Deng Y, Raabe D and Tasan C C 2016 *Nature* **534** 227

[110] Ye Y F, Wang Q, Lu J, Liu C T and Yang Y 2016 *Mater. Today* **19** 349

[111] Shafeie S, Guo S, Hu Q, Fahlquist H, Erhart P and Palmqvist A 2015 *J. Appl. Phys.* **118** 184905

[112] Zhao F, Wang H, Wu Y, Liu X and Lu Z 2017 *Mater. Res. Lett.* **5** 187

[113] Moure A, Rull-Bravo M, Abad B, Del Campo A, Rojo M M, Aguirre M H, Jacquot A, Fernandez J F and Martin-Gonzalez M 2017 *Nano Energy* **31** 393

[114] Jiang Q, Yang J, Xin J, Zhou Z, Zhang D and Yan H 2017 *J. Alloys Compd.* **694** 864

[115] Cederkrantz D, Farahi N, Borup K A, Iversen B B, Nygren M and Palmqvist A E C 2012 *J. Appl. Phys.* **111** 023701

[116] Zhou Z, Yang J, Jiang Q, Zhang D, Xin J, Li X, Ren Y and He X 2017 *J. Am. Ceram. Soc.* **100** 5723

[117] Dou Y C, Qin X Y, Li D, Li L L, Zou T H, and Wang Q Q 2013 *J. Appl. Phys.* **114** 044906

[118] Nandihalli N, Guo Q, Gorsse S, Khan A U, Mori T and Kleinke H 2016 *Eur. J. Inorg. Chem.* **6** 853

[119] Zhou X, Wang G, Guo L, Chi H, Wang G, Zhang Q, Chen C, Thompson T, Sakamoto J, Dravid V P, Cao G and Uher C 2014 *J. Mater. Chem. A* **2** 20629

[120] Tan G, Shi F, Hao S, Zhao L D, Chi H, Zhang X, Uher C, Wolverton C, Dravid V P and Kanatzidis M G 2016 *Nat. Commun.* **7** 12167

[121] Zhang J, Wu D, He D, Feng D, Yin M, Qin X and He J 2017 *Adv. Mater.* **29** 1703148

[122] Fu L, Yin M, Wu D, Li W, Feng D, Huang L and He J 2017 *Energy. Environ. Sci.* **10** 2030

[123] Meng X, Liu Z, Cui B, Qin D, Geng H, Cai W, Fu L, He J, Ren Z and Sui J 2017 *Adv. Energy Mater.* **7** 1602582

[124] Kim S I, Lee K H, Mun H A, Kim H S, Hwang S W, Roh J W, Yang D J, Shin W H, Li X S, Lee Y H, Snyder G J and Kim S W 2015 *Science* **348** 109

[125] Chen Z, Jian Z, Li W, Chang Y, Ge B, Hanus R, Yang J, Chen Y, Huang M, Snyder G J and Pei Y 2017 *Adv. Mater.* **29** 1606768

[126] Zhang Q, Liao B, Lan Y, Lukas K, Liu W, Esfarjani K, Opeil C, Broido D, Chen G and Ren Z 2013 *Proc. Natl. Acad. Sci. USA* **110** 13261

[127] Tan G, Shi F, Hao S, Chi H, Zhao L D, Uher C, Wolverton C, Dravid V P and Kanatzidis M G 2015 *J. Am. Chem. Soc.* **137** 5100

[128] Yang H, Bahk J H, Day T, Mohammed A M, Snyder G J, Shakouri A and Wu Y 2015 *Nano lett.* **15** 1349

[129] Xu B, Agne M T, Feng T, Chasapis T C, Ruan X, Zhou Y, Zheng H, Bahk J H, Kanatzidis M G, Snyder G J and Wu Y 2017 *Adv. Mater.* **29** 1605140

[130] Cabrera H, Zumeta-Dubé I, Korte D, Grima-Gallardo P, Alvarado F, Aitken J A, Brant J A, Zhang J H, Calderónc A, Marínc E, Aguilar-Frutis A, Erazo J E, Perez-Cappe E and Frankod M 2015 *J. Alloys Compd.* **651** 490

[131] Kumar A, Dhama P, Saini D S and Banerji P 2016 *RSC Adv.* **6** 5528

[132] Chakrabarti D J and Laughlin D E 1983 *Bull. Alloys Pha. Diagr.* **4** 254

[133] Dennler G, Chmielowski R, Jacob S, Capet F, Roussel P, Zastrow S, Nielsch K, Opahle I and Madsen G K 2014 *Adv. Energy Mater.* **4** 1301581